

# $^6\text{Li}$ in the atmosphere of GJ 117 Revisited

D.J. Christian<sup>1</sup> M. Mathioudakis,

*Astrophysics Research Centre, Queen's University Belfast, Belfast, BT7 1NN, Northern Ireland, U.K.*

and

D. Jevremović

*Astronomical Observatory, Volgina 7, 11160 Belgrade, Serbia and Montenegro*

## ABSTRACT

Detection of  $^6\text{Li}$  has been shown for energetic solar events, one chromospherically active binary, and several dwarf halo stars. We had previously found a  $\frac{^6\text{Li}}{^7\text{Li}} = 0.03 \pm 0.01$  for active K dwarf GJ 117 using VLT UVES observations. Here we present high signal-to-noise ( $>1000$ ) high spectral resolution observations taken with the McDonald Observatory's 2.7m and echelle spectrometer of GJ 117. We have used the solar spectrum and template stars to eliminate possible blends, such as Ti I, in the  $^6\text{Li}$  spectral region. Our new analysis, using an updated PHOENIX model atmosphere finds  $\frac{^6\text{Li}}{^7\text{Li}} = 0.05 \pm 0.02$ . Additionally, bisector analysis showed no significant red asymmetries that would affect the lithium line profile. No changes above the statistical uncertainties are found between the VLT and McDonald data. The amount of  $^6\text{Li}$  derived for GJ 117 is consistent with creation in spallation reactions on the stellar surface, but we caution that uncertainties in the continuum level may cause additional uncertainty in the  $^6\text{Li}$  fraction.

*Subject headings:* Stars: activity – Stars: atmospheres – Stars: individual: GJ 117 – Stars: late-type

---

<sup>1</sup>Current address: Department of Physics and Astronomy, California State University, Northridge, 18111 Nordhoff Street, Northridge, CA 91330

## 1. Introduction

The destruction of primordial lithium in low-mass stars occurs during the pre-main-sequence state and little or no Li is therefore expected in these objects when they arrive on the main sequence. Studies of open clusters found that the largest lithium abundances occur for the fastest rotating stars (Soderblom et al. 1993). This result is in contradiction to the expectation that fast rotation enhances the mixing process that leads to increased lithium depletion, and the rotational history must play an important role in the mixing process (Pinsonneault 1997).

One of the key assumptions in the models of Li depletion, is that lithium can not be produced on the surface of late-type stars and its abundance will only decrease as a function of time. However, if lithium can be produced on the stellar surface, a "quasi-equilibrium" abundance would be reached which could depend on the activity level. Thus, we have been investigating if  ${}^6\text{Li}$  can be formed in active stars by spallation in stellar flares as a result of their high levels of activity.

The presence of  ${}^6\text{Li}$  in metal poor halo stars sparked much debate in the early 1990s (Smith et al. 1993). Subsequent observations confirmed the detection of  ${}^6\text{Li}$  in such halo stars and its production was attributed to formation by cosmic ray spallation in the ISM (Smith et al. 1998; Hobbs & Thorburn 1997), although more recent work argues for a pre-Galactic origin (Asplund et al. 2006).

The detection of  ${}^6\text{Li}$  enhancement has been reported during an energetic flare on a chromospherically active binary (Montes & Ramsey 1998), and an active K dwarf (Christian et al. 2005). There are also indications that this isotope may be enhanced in sunspots (Giampapa 1984; Ritzenhoff et al. 1997). The generation of significant  ${}^6\text{Li}$  in stellar and solar flares has been predicted by several authors (Canal et al. 1975; Walker et al. 1985; Livshits 1997). Such enhanced  ${}^6\text{Li}$  abundances should also be expected for stellar objects if extreme energetic conditions are met (see Mullan & Linsky 1999).

In an earlier paper we have shown the detection of  ${}^6\text{Li}$  in the atmosphere of the active K dwarf GJ 117 (=HD 17925) at the 3% level (Christian et al. 2005). Given the significance of this result we have decided to re-observe GJ 117 at a much higher signal-to-noise than observed so far. Our observations, analysis, and models (which are given in more detail in Christian et al. (2005)) are presented in § 2. Our results are discussed in § 3 with concluding remarks presented in § 4.

## 2. Observations & Data Analysis

### 2.1. Observations

Observations of GJ 117 were conducted between 03 – 09 November 2006 using 107 inch Harlan J. Smith telescope and echelle spectrograph at McDonald Observatory. The CS21-e1 instrument was used with the E1 grating centered at 6708Å and the TK3 2k×2k CCD. This set-up provided a resolution of  $\approx$ 130,000. Multiple exposure of GJ 117 were taken for a combined spectrum with 55 ksec of exposure and a signal-to-noise of over  $\approx$ 1300. The data were reduced with standard IRAF tasks, IMRED.CCDRED and TWODSPEC.APEXTRACT, and further analysis carried out using IDL and the STARLINK based DIPSO software. The spectrum of GJ 117 compared to the solar spectrum (taken with the same set-up) in the Li I 6708Å region is shown in Figure 1.

We also obtained Extreme Ultraviolet Explorer (EUVE) data from the Multimission Archive at Space Telescope. EUVE observed GJ 117 for nearly 200 ksec in December 1994 with a mean count rate in the Deep Survey (DS) 100 Å bandpass of 0.09 counts  $s^{-1}$ . We reduced the EUVE data with the standard IRAF EUV reduction tasks and constructed light curves for the DS data using the XRAY.XTIMING package as discussed previously in Christian et al. (1998). A log of the GJ 117 observations are listed in Table 1.

### 2.2. Model Spectra

$^6$ Li is separated from the  $^7$ Li doublet only by 0.16 Å and has a strength typically less than a few percent of that feature. In addition to the feature's intrinsic weakness, the situation is further complicated by blending with nearby lines, such as CN, Fe I, and Ti I (Nissen et al. 1999; Reddy et al. 2002). Contamination by such lines becomes more prevalent as we move down the main sequence to cooler metal-rich stars. Template stars were observed along with GJ 117 to try to resolve the issue of blending. These stars were chosen to have a  $\log(T)$  similar to GJ 117, and of the several observed, GJ 211 (HD 37394) also has the closest metallicity ( $Fe/H = 0.12$ ), compared to GJ 117 ( $Fe/H=0.15$ ; Luck & Heiter (2005)). The spectra of GJ 211 and GJ 117 are compared in Figure 2. CN lines near 6707.5 that have been seen to be  $\leq 1$  mÅ in the solar spectrum, are also very weak in GJ 211, with an equivalent width upper limit of  $\approx 0.5$  mÅ. CN should have a negligible effect on the GJ 117 Li I line profile. Additionally there is no evidence for a strong Ti I line near 6708.025 Å with a conservative upper limit of  $\leq 1$  mÅ.

The general stellar atmosphere code PHOENIX (see Hauschildt et al. 1995; Allard & Hauschildt

Table 1. OBSERVATION LOG

Name	Observation Date	Exposure (sec)	Air Mass
McDonald			
GJ 117 <sup>a</sup>	2006 Nov 04	1800	1.44
		1800	1.39
		1800	1.38
		1800	1.39
		1800	1.56
	2006 Nov 05	1800	1.45
		2500	1.39
		2500	1.38
		2000	1.65
	2006 Nov 06	1800	1.49
		3000	1.42
		3000	1.38
	2006 Nov 07	3000	1.39
		1800	1.48
	2006 Nov 08	1800	1.68
		3000	1.52
		1800	1.86
	2006 Nov 09	1800	1.42
		3000	1.38
		1800	1.46
GJ 211 <sup>b</sup>	2006 Nov 04	900	1.13
		1800	1.65
	2006 Nov 05	900	1.10
		900	1.11
	2006 Nov 06	1200	1.15
EUV			
GJ 117	1994 Dec 02	192 <sup>c</sup>	...

<sup>a</sup>GJ 117: RA<sub>J2000</sub>= 02 52 32.1; Dec<sub>J2000</sub>= -12 46 11.0

<sup>b</sup>Stellar template (see text).

<sup>c</sup>EUV observation time in kiloseconds.

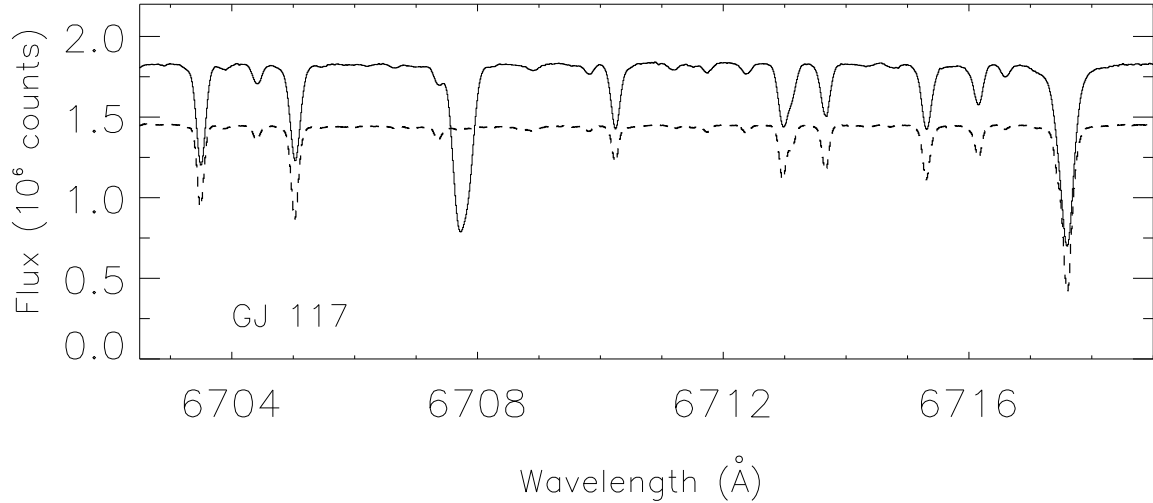


Fig. 1.— McDonald echelle spectra of GJ 117 (solid histogram) compared to the solar spectrum (dashed line) in the Li I 6707.8 $\text{\AA}$  region. The spectra are shown in total counts and the solar spectrum is offset by 30% for ease of presentation.

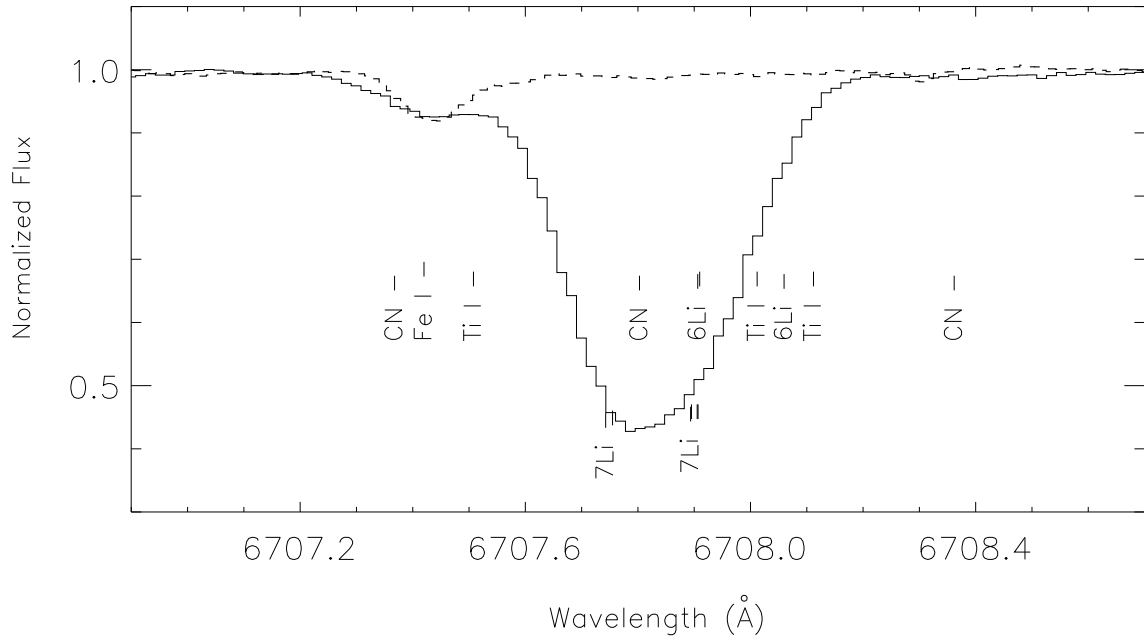


Fig. 2.— Comparison of the McDonald GJ 117 spectrum (solid histogram) to that of a K2 template star, GJ 211 (dashed line).

1995) was used to calculate theoretical stellar spectra. We have used the PHOENIX NextGen series LTE atmosphere models (Hauschildt, Allard, & Baron 1999) for the effective temperature ( $\log(T_{\text{eff}})=3.7$ ) and gravity ( $\log(g)=4.6$ ) of GJ 117 (Gray 2005; Cincunegui et al. 2007). We constructed a grid of models from NextGen that sampled every 200K in  $T_{\text{eff}}$  and 0.5dex in  $\log(g)$ . Direct opacity sampling (Hauschildt et al. 2001) is used within PHOENIX to handle any line blanketing, where the opacity at each wavelength point is calculated as a sum of opacities from all the contributing species. We added the  ${}^6\text{Li}$  resonance doublet to the PHOENIX master line list (Kurucz 1995) using the wavelengths and  $gf$  values of Smith et al. (1993). A Ti abundance of  $\log(\text{Ti}) = 5.22$  was chosen from Luck & Heiter (2005). We caution that the Ti abundance and  $\frac{{}^6\text{Li}}{{}^7\text{Li}}$  ratio are anti-correlated and increasing the Ti abundance decreases the  $\frac{{}^6\text{Li}}{{}^7\text{Li}}$  ratio and conversely, decreasing the Ti abundance increases the  $\frac{{}^6\text{Li}}{{}^7\text{Li}}$  ratio.

Model spectra were calculated with a microturbulence velocity of  $\xi=1.5 \text{ km s}^{-1}$ . This value is typical for solar-type stars and is consistent with the microturbulence given for GJ 117 in Allende Prieto et al. (2004). We derived a  $vsini$  of GJ 117 of  $5.5\pm0.2 \text{ km s}^{-1}$  using  $\chi^2$  analysis of several lines in the Li I 6707.8Å region (Christian et al. 2005). We show model fits for the Fe I  $\lambda 6713.7$  and Ca I at  $\lambda 6717.685$  line profiles in Figure 3 using the derived  $vsini$  of  $5.5 \text{ km s}^{-1}$ .

Reddy et al. (2002) have shown that the apparent detection of  ${}^6\text{Li}$  for planet hosting star HD 82943 could be explained by the presence of Ti I lines near 6708.03 and 6708.1 Å. Although our template spectrum of GJ 211 rules out any strong Ti I features in the red-side of the lithium line profile we constructed a second set of PHOENIX models (PHX2) with the Ti I values of Reddy et al. (2002) for comparison and completeness. We show the line list for important lines in the vicinity of the lithium line profile and their comparison to Reddy et al. (2002) in Table 2. This second PHOENIX model (PHX2) has the same values as shown for the first PHOENIX model in Table 2, but includes the Reddy et al. (2002) values for the Ti lines at 6707.752, 6708.025 and 6708.125 Å.

Bisector analysis has been shown to be useful in disentangling subtle enhancements in line profiles that may be caused by blending with weaker lines and indicate other effects in the stellar atmosphere, such as granulation. In a recent paper, Cayrel et al. (2007) have used bisector analysis in observed line profiles of HD 74000 and have shown that previously undetected line asymmetries may cause derived lithium fractions to be lower than previously reported. We have performed bisector analysis on 3 Fe lines (6703.5, 6705.1, 6713.7Å) in the Li 6708Å region to evaluate the effect of asymmetries. We show the line bisectors for 2 of these Fe lines in Figure 4. We find that the line bisectors for these lines on GJ 117 are vertical, and show a blue asymmetry near the top of the profile, but show no red-symmetry. We estimate an upper limit to red-asymmetry of  $\approx 0.005 \text{ Å}$  (0.2 km/s). This is consistent

Table 2. Lines in the vicinity of the Li I 6707.8 Å profile

Wavelength	Element	LEP (eV)		log gf	
		Å	R02 <sup>a</sup>	PHX <sup>a</sup>	R02
6707.3810	CN	1.83	1.83	−2.170	−2.141
6707.4330	Fe I	4.61	4.61	−2.283	−2.283
6707.4500	Sm II	0.93	0.93	−1.040	−2.379
6707.4640	CN	0.79	0.78	−3.012	−2.921
6707.5210	CN	2.17	2.00	−1.428	−1.358
6707.5290	CN	0.96	0.96	−1.609	−1.594
6707.5630	V I	2.74	2.74	−1.530	−1.995
6707.6440	Cr I	4.21	4.21	−2.140	−2.667
6707.7520	Ti I	4.05	4.77	−2.654	−2.656
6707.7610 <sup>b</sup>	<sup>7</sup> Li	0.00	0.00	−0.002	−0.009
6707.7710	Ca I	5.80	5.79	−4.015	−4.014
6707.8160	CN	1.21	1.21	−2.317	−1.967
6707.9130 <sup>c</sup>	<sup>7</sup> Li	0.00	0.00	−0.807	−0.309
6707.9210	<sup>6</sup> Li	0.00	0.00	−0.002	−0.005
6708.0250	Ti I	1.88	...	−2.252	...
6708.0728	<sup>6</sup> Li	0.00	0.00	−0.303	−0.309
6708.0940	V I	1.22	1.22	−3.113	−3.113
6708.1250	Ti I	1.88	5.65	−2.886	−2.801
6708.3750	CN	2.10	1.89	−2.252	−1.959

<sup>a</sup>R02 – from the line list of Reddy et al. (2002); PHX – from the PHOENIX line list used in this work.

<sup>b</sup>Ave of  $\lambda\lambda$ 6707.754 and 6707.766 <sup>7</sup>Li lines

<sup>c</sup>Ave of  $\lambda\lambda$ 6707.904 and 6707.917 <sup>7</sup>Li lines

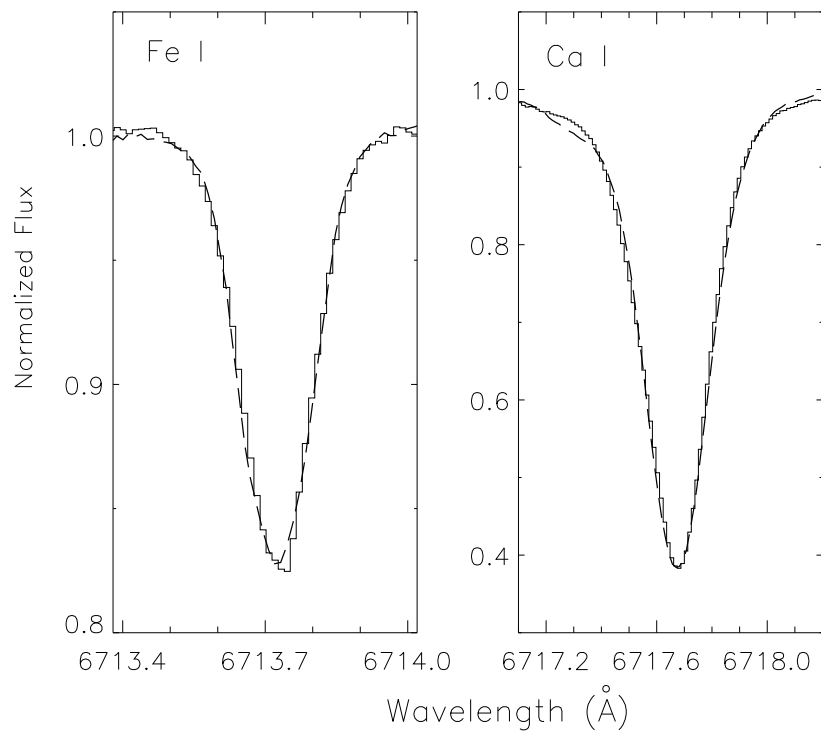


Fig. 3.— Sample synthetic line profiles for: Fe I  $\lambda$ 6713.7 (left), and Ca I  $\lambda$ 6717.68 (right) lines using the derived  $v\sin i$  of  $5.5 \text{ km s}^{-1}$  (see text).

with our earlier estimates from VLT UVES spectra of GJ 117. We therefore conclude, that there are no significant red asymmetries that may affect the Li line profile. We discuss uncertainties in continuum placement in Section 3.1, which compares the McDonald and VLT spectra of GJ 117.

### 3. Results & Discussion

#### 3.1. The $\frac{^6Li}{^7Li}$ isotope ratio

We have compared the combined McDonald spectrum to the PHOENIX models using a least square fitting technique where the quality of the fit is determined by  $\chi^2$  statistics (Christian et al. 2005; Smith et al. 1998).

$$\chi_r^2 = \frac{1}{dof} \sum_1^n \frac{(D_i - M_i)^2}{\sigma_i^2} \quad (1)$$

where  $D_i$  and  $M_i$  are the data and model fluxes at data point  $i$ , respectively. We defined the variance,  $\sigma_i$  as the square root of the counts at each wavelength.  $\sigma$  ranged from  $\approx 900$  in the lithium line center to  $\approx 1350$  in the continuum. The standard continuum normalization was determined using the DIPSO CREGS routine for continuum placement. We performed a least-squares fitting to check this continuum level. We selected 0.3 Å regions of continuum to the blue and red side the  $^7Li$  line profile. We fitted the model against the data and adjusting the data by a normalization factor between 0.98 and 1.02 in 0.001 increments, and determined a minimum  $\chi^2$  for a normalization factor of 1.003. We then used this normalization factor in fitting each PHOENIX  $^6Li$  model to the data by varying the  $\frac{^6Li}{^7Li}$  fraction in 0.01 increments. In this way the most probable model with  $\chi^2 \sim 1$  was determined.  $\chi^2$  was computed over the red-side of the  $^6Li + ^7Li$  line profile in the wavelength range of 6707.65 to 6708.35 Å, giving 54 degrees of freedom (dof). We show the combined McDonald spectrum and its comparison to 3 models with the  $\frac{^6Li}{^7Li}$  fraction ranging from 0.0, 0.05, and 0.10 in Figure 5a, and an expanded view of the red-side of the lithium line profile in Figure 5b. The best fitting model had a  $\frac{^6Li}{^7Li} = 0.05$  with a  $\chi^2$  of  $\approx 58$  and the model with no  $^6Li$  had a  $\chi^2 \approx 284$ . We show the reduced  $\chi^2$  values for each model and Table 3. For the residuals Figures 5ab we include a sign factor to  $\chi^2$  to indicate whether the observational data was larger than (positive) or smaller than (negative) the model.

We computed the F-statistic and compared the reduced  $\chi^2$  for each model to the model with the minimum reduced  $\chi^2$  (model with  $\frac{^6Li}{^7Li} = 0.05$ ), and show this in Figure 6. For 54 degree of freedom the 90% confidence limit for the F ratio is  $\approx 2.8$  and this ratio is also

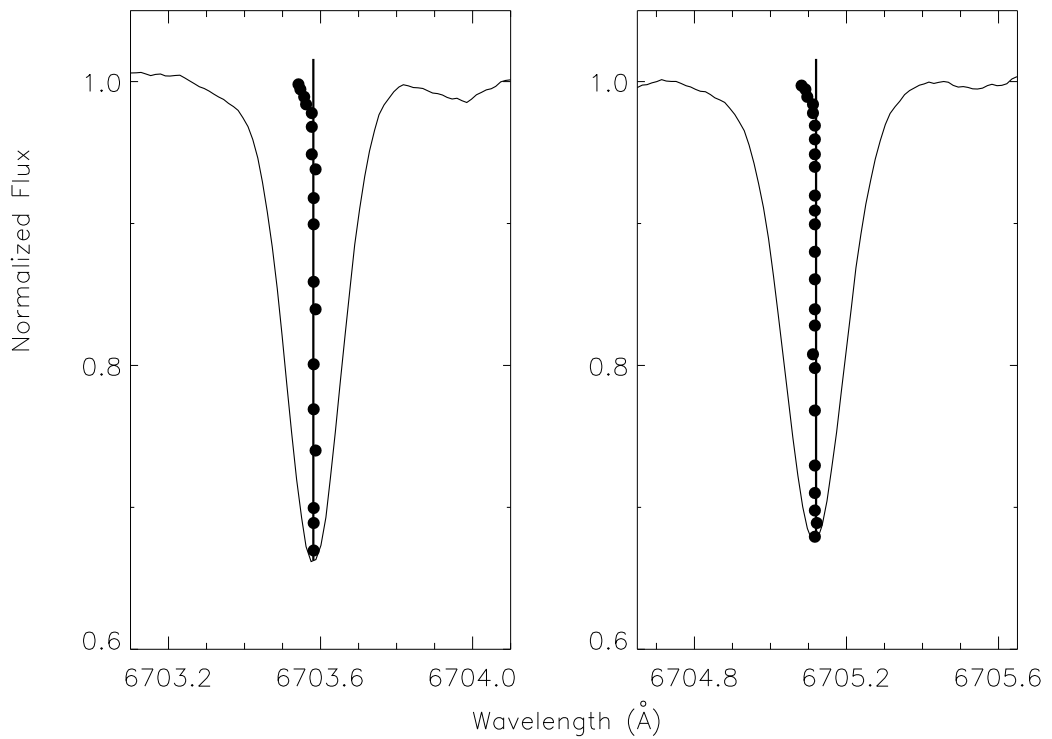


Fig. 4.— Sample line bisectors for 2 Fe I lines ( $\lambda 6703.5$  &  $\lambda 6705.1$ ) in the vicinity of the lithium line profile.

shown in Figure 6. The  $1\sigma$  uncertainty of the  ${}^6\text{Li}$  fraction is 0.02, giving  $\frac{{}^6\text{Li}}{{}^7\text{Li}} = 0.05 \pm 0.02$ .

Recently, Cayrel et al. (2007) cautioned that the continuum placement and the uncertainty in the continuum level may dominate the errors in the  ${}^6\text{Li}$  fraction, and we tested the effect on the this level on the  ${}^6\text{Li}$  fraction. We find that a normalization of 1.01 (1% increase in the continuum level derived a  $\frac{{}^6\text{Li}}{{}^7\text{Li}} = 0.03$  when re-fitting the lithium line, but clearly does not fit the line center (data now higher than the model) and this fit has  $\chi^2$  about 60 higher than the best fit normalization of the continuum, which gives  $\frac{{}^6\text{Li}}{{}^7\text{Li}} = 0.05$ . Conversely, by lowering the continuum fraction by 1%, we find a  $\frac{{}^6\text{Li}}{{}^7\text{Li}} = 0.06$ , but again this shows an overall poor fit to the line and continuum and has  $\chi^2$  about 100 higher than the best fit normalization of the continuum.

We also investigated if small wavelength shifts could change the derived  $\frac{{}^6\text{Li}}{{}^7\text{Li}}$  fraction. Our PHOENIX models are generated with a wavelength increment of 0.01 Å and then re-binned and interpolated onto the observed wavelength scale. Thus any small shifts caused by an uncertainty in the wavelength scale should be accounted for as the data and model shift relative to each other. However, we tested how small absolute shifts between the data and model would change  $\chi^2$  and the derived  $\frac{{}^6\text{Li}}{{}^7\text{Li}}$ . Shifts to the data relative to the model on the order of 1% of a resolution element (0.5 mÅ) only changed  $\chi^2$  by a small amount and caused no changes to the computed  $\frac{{}^6\text{Li}}{{}^7\text{Li}}$ . However, we then tested what amount of an absolute shift would cause a change of 0.01 in the  $\frac{{}^6\text{Li}}{{}^7\text{Li}}$ . A shift of +5mÅ (10% of a resolution element) is needed to shift the best fitting model for the  $\frac{{}^6\text{Li}}{{}^7\text{Li}}$  to 0.06 and similarly a shift of -5 mÅ gives the best fitting model to 0.04. However, both of these shifts produce a  $\chi^2$  approximately 30 higher than the best fitting model, and such a large shift is not supported by the wavelength calibration and modelling, and any smaller shifts are accounted for in the current uncertainty.

We have found a  $\frac{{}^6\text{Li}}{{}^7\text{Li}}$  of  $0.05 \pm 0.02$  for our McDonald observations of GJ 117. This value is  $\approx 3\%$  higher than our earlier VLT estimate. The main difference can be attributed to not including the strong Ti I line at 6708.025 Å. If we include this line at the strength used by Reddy et al. (2002) we find a  $\frac{{}^6\text{Li}}{{}^7\text{Li}}$  of  $0.02 \pm 0.01$ . The fitting results for this model are also summarized in Table 3. Our template star, GJ 211 and other K2 stars in our sample do not show any additional absorption near this wavelength stronger than 1 mÅ and our original PHOENIX model appears to be more consistent with GJ 117. An analysis of the VLT spectrum with our first PHOENIX model also finds a similar result for the  $\frac{{}^6\text{Li}}{{}^7\text{Li}}$  of  $0.05 \pm 0.03$  and is thus consistent with our higher signal-to-noise McDonald data. The spectra from the two epochs do not show a significant change above the statistical uncertainties and uncertainty in normalizing the spectra. We note that the VLT spectra have a S/N of  $\approx 400$ , significantly lower than the McDonald observations.

Table 3. Results for  $\chi_r^2$  for PHOENIX model fitting

$\frac{^6Li}{^7Li}$	$\chi_r^2$ PHX <sup>a</sup>	$\chi_r^2$ PHX2 <sup>b</sup>
0.00	5.27	1.70
0.01	3.52	1.18
0.02	2.29	0.98
0.03	1.56	1.11
0.04	1.14	1.45
0.05	1.08	2.06
0.06	1.42	3.01
0.07	2.15	4.01
0.08	3.01	5.36
0.09	4.42	6.88
0.10	6.09	8.76

<sup>a</sup>PHX – from the PHOENIX line list used in this work.

<sup>b</sup>PHX2 model with additional Ti I from the line list of Reddy et al. 2002

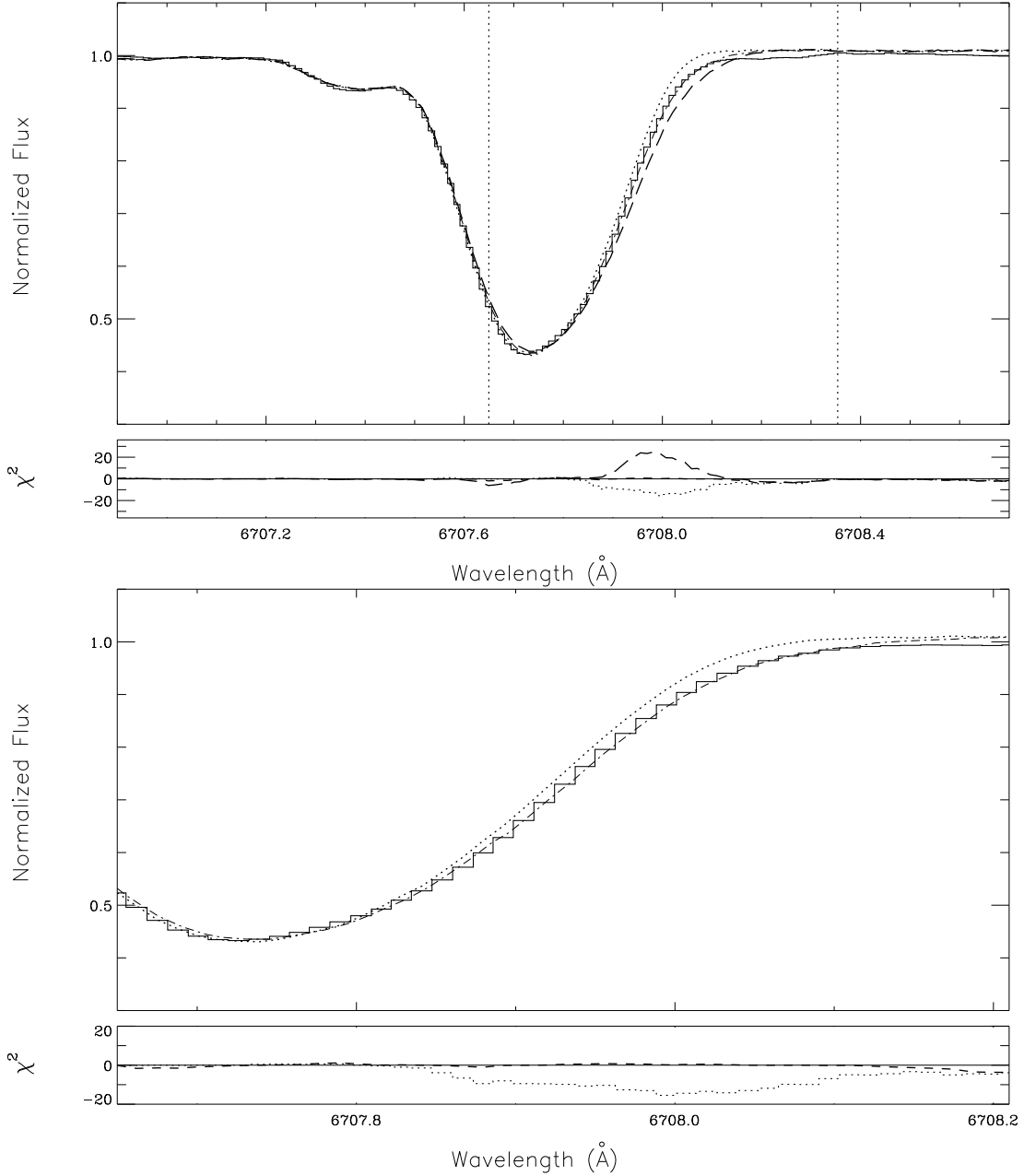


Fig. 5.— GJ 117 spectrum for the Li I 6707.8 Å region plotted as a solid histogram. a. (top-figure) Over-plotted are PHOENIX models with  $\frac{6Li}{7Li}$  ratios of 0.0 (dotted), 0.05 (dash-dotted), and 0.10 (long-dashed) lines. The lower panel shows  $\chi^2$  residuals from the difference of the data minus the model (see text). The interval in which  $\chi^2$  was calculated is indicated by the dotted vertical lines. b. (bottom-figure) Shows an expanded view of the lithium line profile with only the PHOENIX models with  $\frac{6Li}{7Li}$  ratios of 0.0 (dotted), 0.05 (dash-dotted) over-plotted, and their residuals.

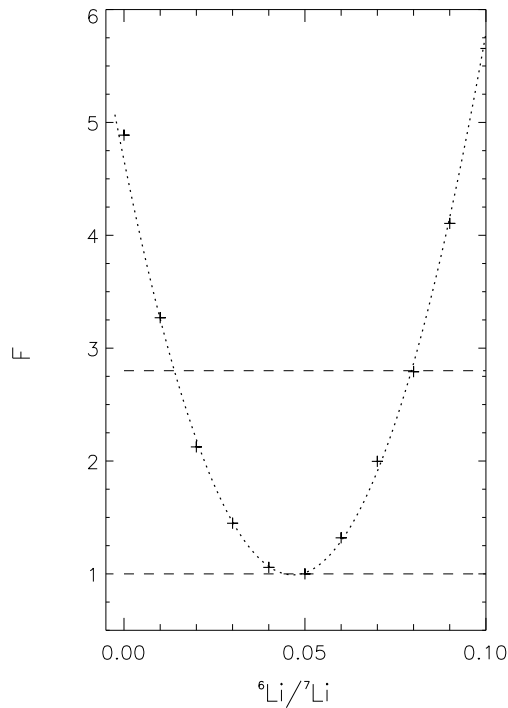


Fig. 6.— The F statistic as a function of the  $\frac{^6\text{Li}}{^7\text{Li}}$  ratio for Li model line profiles as compared to the observations for GJ 117. F is defined as the ratio of reduced  $\chi^2$  for each model to the model with the minimum reduced  $\chi^2$ . The F value for a 90% confidence limit ( $\approx 2.80$ ) is over-plotted as the dashed horizontal line. A F value of 1 is also indicated.

### 3.2. Evidence for flare activity on GJ 117

The higher rotational velocity and deeper convection zone make GJ 117 considerably more active than the Sun. In our earlier work (Christian et al. 2005) we presented arguments for the generation of Li in the atmosphere of GJ 117 by spallation reactions (for example, see the recent work of Tatischeff et al. (2008)). These arguments were based on the strong quiescent X-ray luminosity of this source which in turn implied a high time-averaged flare energy (Doyle & Butler 1985).

We have examined archival EUVE data for GJ 117 for variability. A light curve of these observations in the EUVE DS 100Å bandpass is shown in Figure 7. The observations of GJ 117 shows 3 small flares during the 540 ksec duration. The largest flare shows a  $\approx 50\%$  increase over the quiescent rate of 0.09 counts s $^{-1}$ . The variability of GJ 117 was also confirmed found to be significant using the Kolmogorov-Smirnov (KS) statistical tests (Christian et al. 1998).

## 4. Concluding Remarks

We have obtained high resolution McDonald echelle observations of the dK1 star GJ 117 as a follow-up to our detection of  ${}^6\text{Li}$  in this object using VLT and UVES (Christian et al. 2005). Here we report the detection of  ${}^6\text{Li}$  in our McDonald data at the 5% level ( $\frac{{}^6\text{Li}}{{}^7\text{Li}} = 0.05 \pm 0.02$ ). We have used the solar spectrum and template stars to eliminate possible blends, such as Ti I, in the  ${}^6\text{Li}$  spectral region. Additionally, bisector analysis showed no significant red asymmetries that would affect the lithium line profile. GJ 117 is much more active than the Sun and its X-ray luminosity is at least one order of magnitude higher. As outlined in Christian et al. (2005), GJ 117 has the needed energy budget to produce the observed  ${}^6\text{Li}$  in spallation reactions on the stellar surface. However, we caution that uncertainties in the continuum placement may cause additional errors that may decrease or increase the  ${}^6\text{Li}$  fraction for the current methods used. Future high resolution observations during a large flare event on such Li-rich active dwarf stars could provide definitive proof of spallation reactions in these stars.

We thank David Doss and all of the McDonald staff for their excellent support for this project. We thank Dr. David Lambert for suggested improvements to the manuscript. We also thank an anonymous referee for suggested improvements. DC thanks STFC for travel support. D.J. was supported by the projects No 146001 and 146007 financed by Ministry of Science of Serbia.

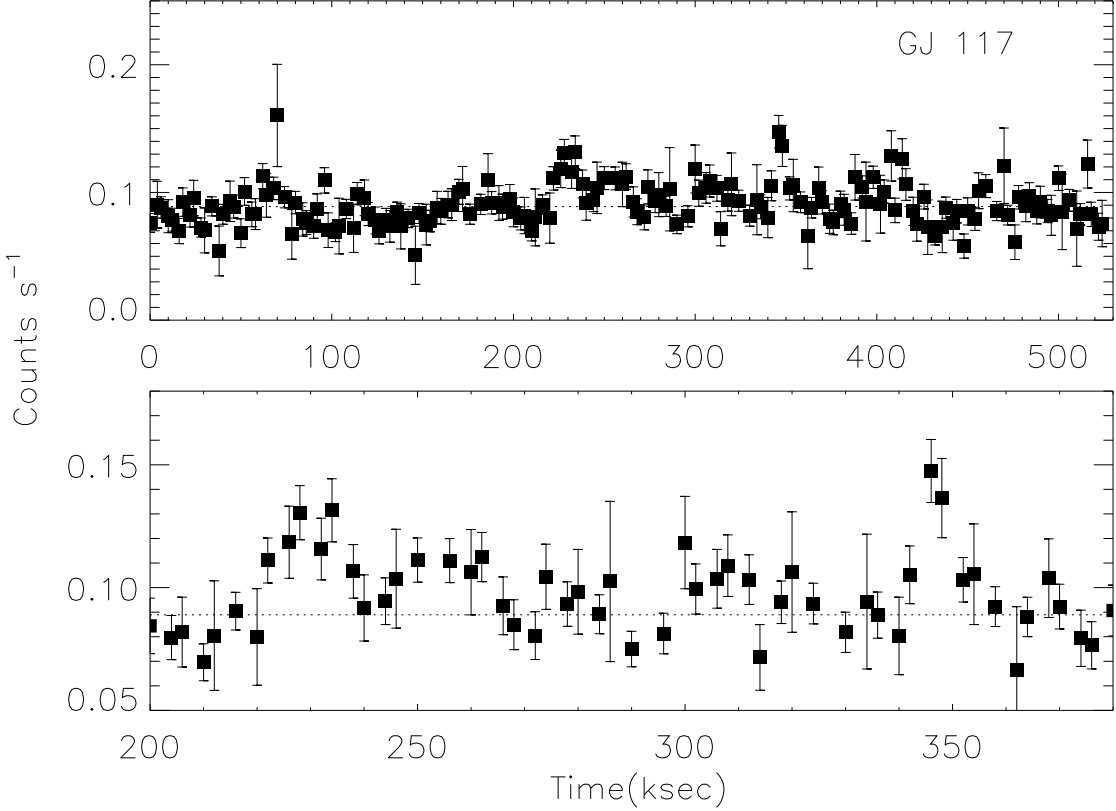


Fig. 7.— EUVE light curve data. The *top* panel shows the entire observation in 2 ksec bins for the Deep Survey 100 Å bandpass. The *lower* panel shows a blow-up of the 200–400 ksec interval showing two flares (see text).

## REFERENCES

Allard, F., Hauschildt, P. H. 1995, ApJ, 445, 433  
Allende Prieto, C., Barklem, P. S., Lambert, D. L., Cunha, K. 2004, A&A, 420, 183  
Asplund, M., Lambert, D.L., Nissen, P.E., Primas, F., Smith, V.V. 2006, ApJ, 644, 229  
Canal, R., Isern, J., & Sanahuja, B. 1975, ApJ, 200, 646  
Cayrel, R. et al. 2007, A&A, in press (arXiv:0708.3819)  
Christian, D.J., Mathioudakis, M., Drake, J.J. 1998, AJ, 115, 316  
Christian, D.J., Mathioudakis, M., Jevremović, D., Hauschildt, P., & Baron, E. 2005, ApJ, 632, L127

Cincunegui, C., Díaz, R. F., Mauas, P.J.D. 2007, A&A, 469, 309

Doyle, J.G., Butler, C.J. 1985, Nature, 313, 378

Giampapa, M., 1984 ApJ, 277, 235

Gray, D. F. 2005, The Observation and Analysis of Stellar Photospheres, 3rd edn., ed. D. F. Gray (Cambridge, UK: Cambridge University Press)

Hauschildt, P. H., Starrfield, S., Allard, F., & Baron, E. 1995, ApJ, 447, 829

Hauschildt, P. H., Allard, F., & Baron, E. 1999, ApJ, 512, 377

Hauschildt, P. H., Lowenthal, David K., Baron, E. 2001, ApJS, 134, 323

Hobbs, L. M. & Thorburn, J. A. 1997, ApJ, 491, 772

Kurucz, R. L. 1995, in ASP Conf. Ser. 78, Astrophysical Applications of Powerful New Databases, ed. S. J. Adelman & W. L. Wiese (San Francisco: ASP), 78, 205

Livshits, M. A. 1997, Sol. Phys., 173, 377

Luck, R.E., & Heiter, U. 2005, AJ, 129, 1063

Montes, D., Ramsey, L.W. 1998, A&A, 340, L5

Mullan, D.J., Linsky, J. 1999, ApJ, 502, 511

Nissen, P.E., Lambert, D.I., Primas, F., & Smith V.V. 1999, A&A, 348, 211

Pinsonneault, M.H. 1997, ARA&A, 35, 557

Reddy, B.E., Lambert, D.L., Laws, C., Gonzalez, G., & Covery, K. 2002, MNRAS, 335, 1005

Ritzenhoff, S., Schröter, E.H., & Schmidt, W. 1997, A&A, 328, 695

Smith, V.V., Lambert, D.I., Nissen, P.E. 1993, ApJ, 408, 262

Smith, V.V., Lambert, D.I., Nissen, P.E. 1998, ApJ, 506, 405

Soderblom, D.R., et. al. 1993, AJ, 106, 1059

Tatischeff, V., Thibaud, J. -P., Ribas, I. 2008, arXiv:0801.1777

Walker, T. P., Mathews, G. J., & Viola, V. F. 1985, ApJ, 745, 751